# Modification of Silica Nanoparticles with 4,6-Diacetylresorcinol as a Novel Composite for the Efficient Removal of Pb(II), Cu(II), Co(II), and Ni(II) Ions from Aqueous Media

Asma S. Al-Wasidi[1] · Ahmed M. Naglah[2,3] · Fawaz A. Saad[4] · Ehab A. Abdelrahman[5]

## Abstract

Due to the danger of heavy metals such as Pb(II), Cu(II), Co(II), and Ni(II) ions to the environment and humans, the world needs to develop new effective adsorbents to get rid of them. Many Schiff bases can form chelates with most heavy metal ions. Hence, loading them on supports like silicon oxide as new composites help to solve the pollution problem. So, in this work, a new composite based on the formation of Schiff base on silica nanoparticles was facilely synthesized. (3-amino-propyl)trimethoxysilane was used to modify silica nanoparticles with silanol groups (Si–OH). Then, the modified silica was then combined with 4,6-diacetylresorcinol to create a new Schiff base/silica composite. XRD, FE-SEM, FT-IR, CHN analyzer, and $N_2$ adsorption/desorption analyzer were used to characterize the synthesized composite. The formation of the Schiff base results in a significant drop in the intensity of the composite XRD peak at $2\Theta = 21.9°$. In addition, the FT-IR bands at 3443 and 1606 $cm^{-1}$ are due to the stretching and bending vibrations of OH and/or C=N, respectively. The FE-SEM images confirmed that the silica has uneven forms while the composite has a flaky surface due to the formation of the Schiff base. According to an elemental analysis of the composite, the percentages of C, H, and N are 15.26, 3.24, and 1.65%, respectively. The produced Schiff base restricts the pores of silica and hence the composite BET surface area and total pore volume were lowered. The synthesized composite was used to remove Pb(II), Cu(II), Co(II), and Ni(II) ions from aqueous solutions with high efficiency. The maximum uptake capacity of the composite toward Pb(II), Cu(II), Co(II), or Ni(II) ions is 107.066, 89.767, 80.580, and 70.972 mg/g, respectively. The adsorption processes of the investigated metal ions were chemical, spontaneous, and well fitted with the Langmuir equilibrium isotherm and pseudo-second-order kinetic model. The synthesized composite can be successfully regenerated and utilized various times in the removal of investigated metal ions from aqueous solutions.

**Keywords** 4,6-diacetylresorcinol · $SiO_2$ nanoparticles · Nanocomposite · Heavy metals · Adsorption

✉ Ehab A. Abdelrahman
dr.ehabsaleh@yahoo.com; ehab.abdelrahman@fsc.bu.edu.eg

1  Department of Chemistry, College of Science, Princess Nourah Bint Abdulrahman University, P.O. Box 84428, Riyadh 11671, Saudi Arabia

2  Department of Pharmaceutical Chemistry, Drug Exploration & Development Chair (DEDC), College of Pharmacy, King Saud University, P.O. Box 2457, Riyadh 11451, Saudi Arabia

3  Peptide Chemistry Department, National Research Centre, Dokki, Cairo 12622, Egypt

4  Department of Chemistry, Faculty of Applied Sciences, Umm Al-Qura University, Makkah 21955, Saudi Arabia

5  Chemistry Department, Faculty of Science, Benha University, Benha 13518, Egypt

## 1 Introduction

An increase in anthropogenic activity has resulted in the release of numerous dangerous compounds into water resources, endangering aquatic ecosystems and the environment [1–5]. Because heavy metal ions are very poisonous, non-degradable, and have a tendency to bioaccumulate and biomagnify as a result of the food chain, they are the most serious contributors to water pollution [6, 7]. Their mere presence in aquatic sources is enough to have a direct or indirect impact on living systems. Heavy metal ions are extremely harmful to both animals and plants in the soil environment, as they are absorbed by plants and eventually reach animals and humans [8, 9]. Metals are necessary for biological function, but their high concentration has a

significant impact on human health. Concentrations below the toxicity range have few side effects, but when they exceed the allowed limits, they become harmful and cause a variety of physiological and cytological effects [10–14]. The excess existence of these metal ions makes them travel out of the primary metabolic pathway and can attach to protein sites other than native binding sites, disrupting the cell cascade and causing toxicity in living things [15]. In the case Pb(II) ions, when the concentration of it is exceeded 0.05 mg/L, it penetrates the protective blood–brain barrier and is proving to be a risk factor for Alzheimer's disease and senile dementia. It also causes neuro-degenerative diseases, lowers intelligence quotient, causes kidney damage, stunts bone growth, behavioral problems, ataxia, stupor, and hyperirritability [16]. In the case of Cu(II) ions, when the concentration of it is exceeded 0.05 mg/L, it causes allergies, adreno-corticol hyperactivity, alopecia, anaemia, autism, arthritis, cystic fibrosis, kidney disorders, haemorrhaging, and diabetes [16]. In the case of Co(II) ions, when the concentration of it is exceeded 2 μg/L, it causes serious health effects on the lungs, including asthma, pneumonia, allergies in addition to bone defects and skin rashes [17]. In the case of Ni(II) ions, when the concentration of it is exceeded 0.2 mg/L, it causes nausea, dermatitis, chronic asthma, human carcinogen, and coughing [18]. Flocculation, precipitation, membrane separation, evaporation, and ion exchange are some of the ways that can be used in the removal process [19–23]. In terms of sensitivity, efficiency, specificity, and selectivity, each approach has its own set of benefits and drawbacks. Adsorption is the method of choice for many of these approaches owing to its inexpensive cost, simple design, and great operability, particularly its high removal efficiency from dilute solutions [24–27]. Activated carbon, zeolites, layered double hydroxide, biomaterials, organic/inorganic composites, carbon nanotubes-based materials, and other adsorbents have all been utilized to remove heavy metals [28–35]. Hossein et al. synthesize chromium-based metal−organic framework/activated carbon and magnetic metal–organic framework composites for the removal of Co(II), Pb(II), and Pd(II) ions from aqueous media [36, 37]. The consequences of water contamination on the environment and humans have motivated scientists to fabricate new adsorbents for removing heavy metal pollutants. The surface of a lot of materials is modified multiple times in order to improve metal ion uptake removal efficiency [28, 29]. Many Schiff bases can form chelates with a lot of heavy metal ions due to the strong attraction of metal ions toward N and O atoms. Hence, loading them on supports like silicon oxide as new composites help to solve the pollution problem. The innovative aspect of this paper comes from the fact that our research group develops a new composite made of silica nanoparticles and Schiff base. (3-aminopropyl)trimethoxysilane interacted with silica nanoparticles that contain silanol groups (Si–OH). Then, the modified silica was combined with 4,6-diacetylresorcinol to obtain a new Schiff base/silica composite. Pb(II), Cu(II), Co(II), and Ni(II) ions were efficiently removed from aqueous media using the produced composite compared with other adsorbents in the literature.

# 2 Experimental

## 2.1 Materials and Reagents

4,6-diacetylresorcinol ($C_{10}H_{10}O_4$), sodium metasilicate pentahydrate ($Na_2SiO_3.5H_2O$), cetyltrimethylammonium bromide ($C_{19}H_{42}BrN$), (3-aminopropyl)trimethoxysilane ($C_6H_{17}NO_3Si$), nitric acid ($HNO_3$), ethanol ($C_2H_6O$), xylene ($C_8H_{10}$), thiourea ($CH_4N_2S$), hydrochloric acid (HCl), sulfuric acid ($H_2SO_4$), nickel(II) chloride hexahydrate ($NiCl_2.6H_2O$), cobalt(II) chloride hexahydrate ($CoCl_2.6H_2O$), potassium chloride (KCl), sodium hydroxide (NaOH), copper(II) chloride dihydrate ($CuCl_2·2H_2O$), ethylenediaminetetraacetic acid disodium salt dihydrate ($C_{10}H_{16}N_2Na_4O_{10}$), and lead(II) nitrate ($Pb(NO_3)_2$) were gotten from Sigma Aldrich Company (Purity = 99.99%) and utilized as received without further purification.

## 2.2 Synthesis of Silica Composite

The $SiO_2$/(3-aminopropyl)trimethoxysilane sample was first synthesized using the method described by Khalifa et al. [28]. The $SiO_2$/(3-aminopropyl)trimethoxysilane sample was then combined with a 150 mL ethanolic solution containing 2 g of 4,6-diacetylresorcinol and refluxed for one day with stirring in the presence of a few drops of concentrated $H_2SO_4$. The $SiO_2$/Schiff base composite was then filtered, washed with ethanol, and dried for one day under vacuum at 50 °C.

## 2.3 Apparatus

An X-ray diffractometer (D8 Advance, Bruker, Billerica, Massachusetts, United States) was used to examine the X-ray diffraction (XRD) patterns of the silica sample and their Schiff base composite using $K_\alpha$ Cu radiations with a wavelength of 0.15 nm. A Fourier transform infrared spectrophotometer (Nicolet, Waltham, Massachusetts, United States) was used to measure the FT-IR spectra of the silica sample and its Schiff base composite. Scanning electron microscopy (SEM, JEOL, SEM-JSM-5410LV, Akishima, Tokyo, Japan) was used to examine the morphologies of the silica sample and its Schiff base composite. A CHN Elemental Analyzer (PerkinElmer, 2400, Waltham, United States) was used for the determination of the CHN precent of the silica composite. A nitrogen gas sorption analyzer (Quantachrome,

NOVA, Boynton Beach, United States) was utilized for the determination of the BET surface area, average pore radius, and total pore volume of the silica sample and its Schiff base composite. The concentration of the examined metal ions in the solution was determined by Inductively Coupled Plasma Atomic Emission Spectrometry (ICP-AES) (PerkinElmer, Waltham, United States).

## 2.4 Removal of Pb(II), Cu(II), Co(II), and Ni(II) Ions from Aqueous Media

The pH values of 50 mL of 150 mg/L Pb(II), Cu(II), Co(II), or Ni(II) solutions were adjusted to several values (pH 2.5–6.5) before the addition of the composite using 0.1 M NaOH or HCl to study the influence of pH of metal ion solution. The composite was then mixed with 0.05 g of each Pb(II), Cu(II), Co(II), or Ni(II) solution and agitated for 220 min. In order to examine the influence of contact time, the pH values of 50 mL of 150 mg/L of Pb(II), Cu(II), Co(II), or Ni(II) solutions were adjusted to 6.5 before the addition of the composite. Afterward, 0.05 g of the composite is mixed with each Pb(II), Cu(II), Co(II), or Ni(II) solution then the mixture was agitated for several times (15–120 min). In order to examine the influence of temperature, the pH values of 50 mL of 150 mg/L of Pb(II), Cu(II), Co(II), or Ni(II) solutions were adjusted to 6.5 before the addition of the composite. Afterward, 0.05 g of the composite is mixed with each Pb(II), Cu(II), Co(II), or Ni(II) solution then the mixture was agitated at several temperatures (298–328 kelvins) for 90 min. In order to examine the influence of initial metal ion concentration, the pH values of 50 mL of 50–200 mg/L of Pb(II), Cu(II), Co(II), or Ni(II) solutions were adjusted to 6.5 before the addition of the composite. Afterward, 0.05 g of the composite is mixed with each Pb(II), Cu(II), Co(II), or Ni(II) solution then the mixture was agitated at 298 kelvins for 90 min. The composite is separated using centrifugation after each of the aforementioned influences has been studied. After that, using Inductively Coupled Plasma Atomic Emission Spectrometry (ICP-AES), the residual concentration of Pb(II), Cu(II), Co(II), or Ni(II) ions in the filtrate is determined.

Equation (1) can be used to calculate the mass of adsorbed Pb(II), Cu(II), Co(II), or Ni(II) ions per gram of composite (Q, mg/g).

$$Q = \left[ C_i - C_e \right] \times \frac{V}{M} \tag{1}$$

Equation (2) can be used to calculate the% removal (% R) of Pb(II), Cu(II), Co(II), or Ni(II) ions.

$$\%R = \frac{C_i - C_e}{C_i} \times 100 \tag{2}$$

$C_i$ (mg/L) represents the initial concentration of Pb(II), Cu(II), Co(II), or Ni(II) ions whereas $C_e$ (mg/L) represents the final concentration of Pb(II), Cu(II), Co(II), or Ni(II) ions. Additionally, V (L) represents the volume of Pb(II), Cu(II), Co(II), or Ni(II) solution whereas M (g) represents the mass used of the composite. In order to examine the influence of desorption, 0.05 g of the composite was agitated with 50 mL of 150 mg/L of Pb(II), Cu(II), Co(II), or Ni(II) solution (pH 6.5) for 90 min. Additionally, the composite was separated utilizing centrifugation then carefully washed with distilled water. The composite which loaded with Pb(II), Cu(II), Co(II), or Ni(II) ions was then stirred for 60 min with 50 mL of 0.45 M of some desorbing solutions (nitric acid, hydrochloric acid, thiourea, and EDTA disodium salt). In order to examine the reusability experiments for four cycles of adsorption/desorption, 0.05 g of the regenerated composite was stirred with 50 mL of 150 mg/L of Pb(II), Cu(II), Co(II), or Ni(II) solution (pH 6.5) for 90 min. It is noteworthy that 0.45 M of EDTA disodium salt is utilized for regenerating the composite after each cycle. Equation (3) can be used to calculate the% desorption (% D).

$$\%D = \frac{100 C_d V_d}{(C_i - C_e) V} \tag{3}$$

$C_d$ (mg/L) represents the concentration of Pb(II), Cu(II), Co(II), or Ni(II) ions that exist in the desorption solution whereas $V_d$ (L) represents the volume of desorbing solution. According to Khalifa et al. [28], the point of zero charge (pH$_{PZC}$) of the composite can be determined as follows: the initial pH value of 0.025 M potassium chloride solutions was adjusted to multiple values ranging from 2 to 12 using 0.1 M NaOH or HCl. Following that, 0.15 g of the composite was mixed with each potassium chloride solution and agitated for 8 h. The composite was also separated using centrifugation, and the filtrate final pH value (pH$_{final}$) was determined. The pH$_{final}$ values were compared to the pH$_{initial}$ values in a graph. The pH$_{pzc}$ is the pH$_{final}$ level at which a typical plateau was achieved [28].

## 3 Results and Discussion

### 3.1 Characterization of the Synthesized Composite

The XRD patterns of silica and their Schiff base composite are shown in Fig. 1A, B, respectively. The results also indicated that the synthesized silica is cristobalite with a tetragonal structure as JCPDS card No. 00-039-1425 indicates [38]. The produced silica average crystallite size is 45.63 nm. The production of the Schiff base, as explained in Scheme 1, is responsible for the significant reduction in the intensity of the composite XRD peak at $2\Theta = 21.9°$. The

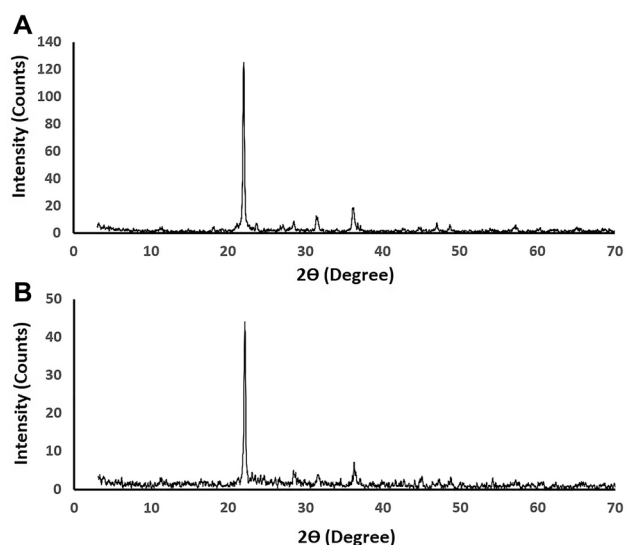**Fig. 1** The X-ray diffraction patterns of the silica (**A**) and their Schiff base composite (**B**)

FT-IR spectra of silica and their Schiff base composite are shown in Fig. 2A, B, respectively. At 466, 620, 790, 1069, 1618, and 3445 cm$^{-1}$, six silica bands can be observed. The bending vibrations of Oxygen-Silicon-Oxygen cause the observed band at 466 cm$^{-1}$. The symmetrical stretching vibrations of Silicon-Oxygen-Silicon are responsible for the observed bands at 620 and 790 cm$^{-1}$. The asymmetrical stretching vibrations of Silicon-Oxygen-Silicon are responsible for the observed band at 1069 cm$^{-1}$. The stretching and bending vibrations of OH cause the bands seen at 3445

and 1618 cm$^{-1}$, respectively [39]. The silica bands in the composite can be observed at 476, 620, 790, 1092, 1606, and 3443 cm$^{-1}$. The stretching and bending vibrations of OH and/or C=N are responsible for the bands detected at 3443 and 1606 cm$^{-1}$, respectively. The stretching vibrations of CH aromatic and CH aliphatic cause the bands at 3006 and 2940 cm$^{-1}$, respectively. The stretching vibrations of C=C aromatic are responsible for the bands observed at 1437, 1476, and 1510 cm$^{-1}$. The bending vibration of CH is responsible for the band observed at 1373 cm$^{-1}$. The out-of-plane bending vibrations of CH aromatic are responsible for the observed bands at 840 and 920 cm$^{-1}$ [40]. Consequently, we conclude from the FT-IR data that all-functional groups of inorganic and organic parts of the synthesized composite existed. Hence, this confirms the proposed structure of the composite as presented in Scheme 1.

According to the elemental analysis of the composite, the percentages of C, H, and N are 15.26, 3.24, and 1.65%, respectively. As a result, the presence of nitrogen and carbon demonstrates that the Schiff base is effectively loaded on the silica as shown in Scheme 1. The FE-SEM images of the silica and their Schiff base composite are shown in Fig. 3A, B, respectively. The results confirmed that the silica has irregular forms whereas the composite has a flaky appearance due to the Schiff base formation. The N$_2$ adsorption/desorption isotherms of silica and their Schiff base composite are shown in Fig. 4A, B, respectively. The results revealed that the obtained isotherms are of type IV [41]. Table 1 contains the values of total pore volume, BET surface area, and average pore size. Because the produced Schiff base restricts the
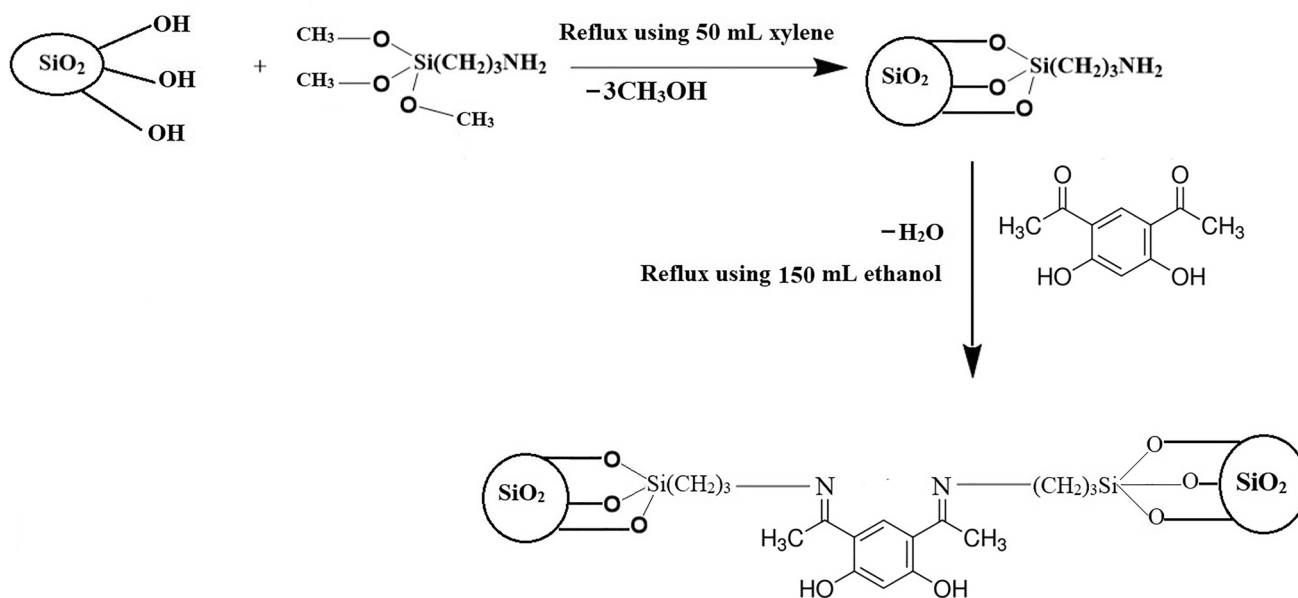
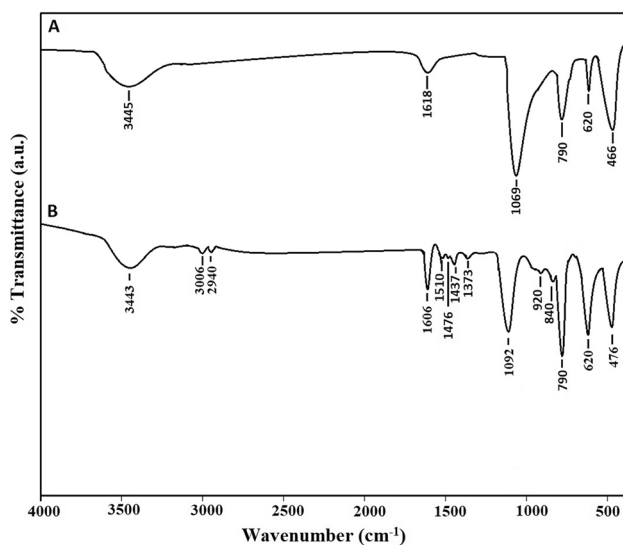

**Scheme 1** The synthetic steps of the composite

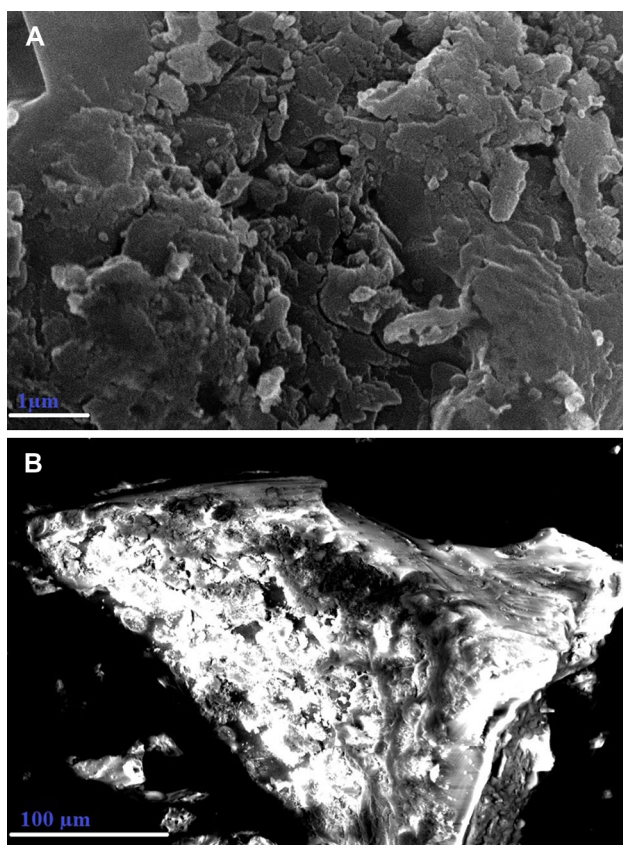**Fig. 2** The FT-IR spectra of the silica (A) and their Schiff base composite (B)



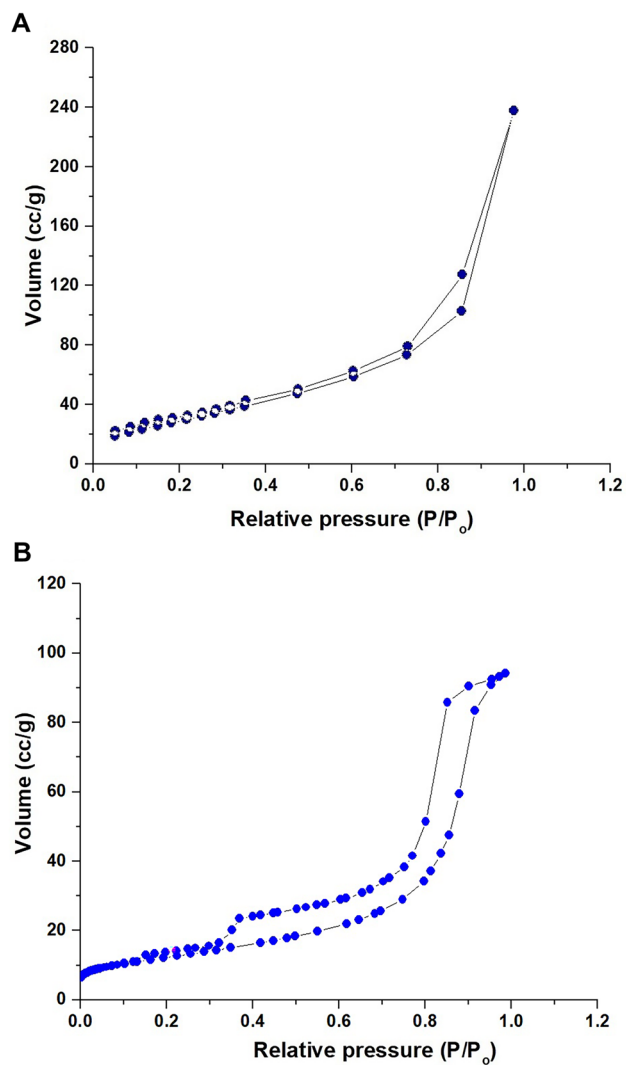**Fig. 3** The FE-SEM images of the silica (**A**) and their Schiff base composite (**B**)



**Fig. 4** The $N_2$ adsorption/desorption isotherms of the silica (**A**) and their Schiff base composite (**B**)

**Table 1** The surface textures of the silica and their Schiff base composite

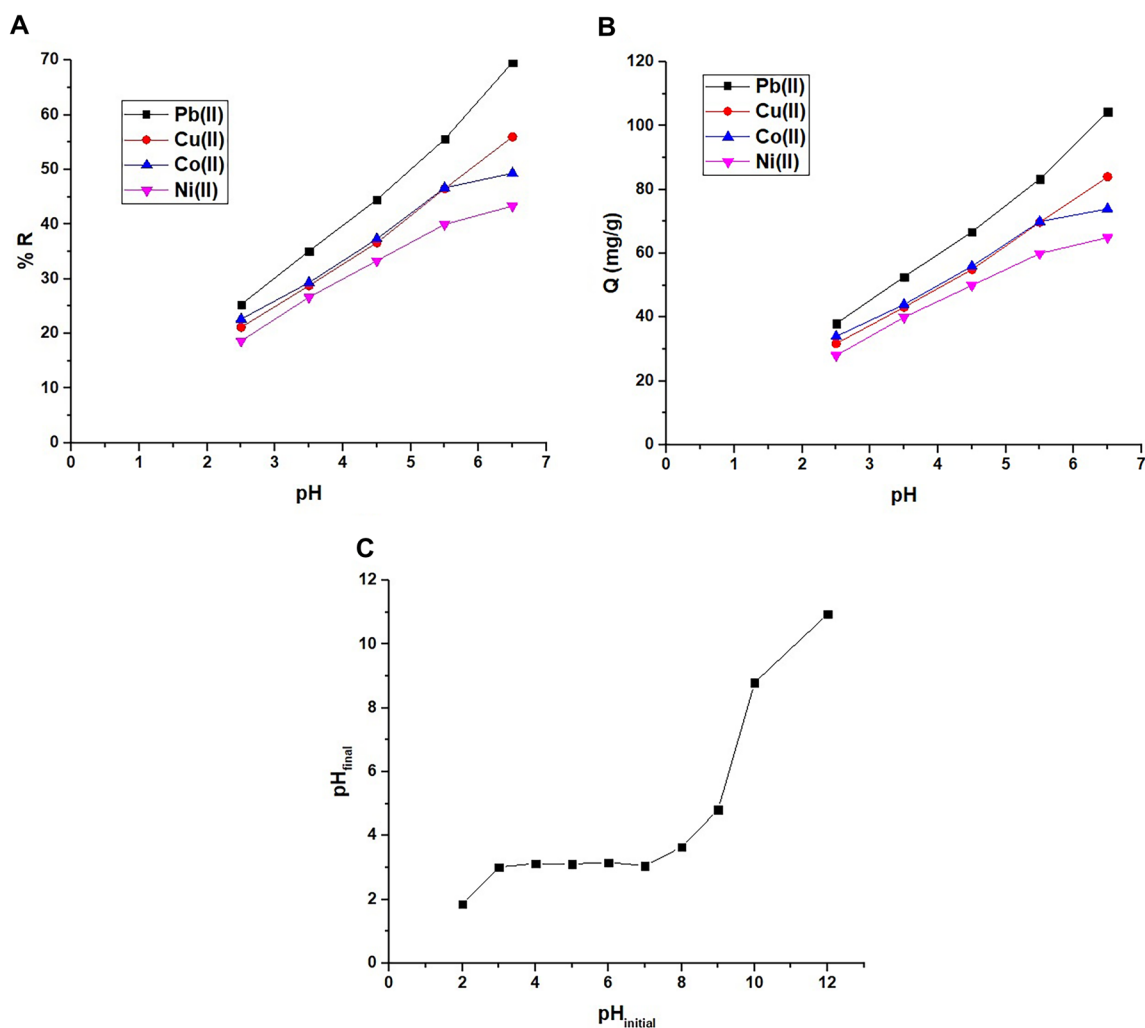| Sample | BET surface area $(m^2/g)$ | Total pore volume (cc/g) | Average pore size (nm) |
|---|---|---|---|
| $SiO_2$ | 110.142 | 0.340 | 6.253 |
| Composite | 44.920 | 0.147 | 0.765 |

**Fig. 5** The effect of pH of the studied metal ion solution on% R (**A**) and Q (**B**). The point of zerocharge of the synthesized composite (**C**)

pores of silica, the composite BET surface area and total pore volume were lowered.

## 3.2 Removal of Pb(II), Cu(II), Co(II), and Ni(II) Ions from Aqueous Media

### 3.2.1 Influence of pH

The effect of pH on% R and Q (mg/g) in the examined metal ion solution is shown in Fig. 5A, B, respectively. The findings revealed that as the pH rises, the% R or Q rises to attain a maximum at pH 6.5.% R of Pb(II), Cu(II), Co(II), and Ni(II) ions at pH 6.5 is 69.61, 56.00, 49.33, and 43.33, respectively. Q of the composite toward of Pb(II), Cu(II), Co(II), and Ni(II) ions at pH 6.5 is 104.42, 84.00, 74.00, and 65.00 mg/g, respectively. The curve of $pH_{final}$ against $pH_{initial}$ for different potassium chloride solutions is shown in Fig. 5C. The results revealed that the composite point

of zero charge is 3.12. In the case of the pH of the Pb(II), Cu(II), Co(II), or Ni(II) solution is less than 3.12, the composite is positively charged because it is surrounded by positive hydrogen ions that repel the investigated metal ions and hence resulting in a decrease in the% R or Q. In the case of the pH of the Pb(II), Cu(II), Co(II), or Ni(II) is more than 3.12, the composite is negatively charged because it is surrounded by negative hydroxide ions which attract the investigated metal ions and hence raise the% R or Q [24, 25].

### 3.2.2 Influence of Contact Time

The effect of the contact time of the examined metal ion solution on% R and Q (mg/g) is shown in Fig. 6A, B, respectively. The results showed that as time goes on, the% R or Q grows, reaching a maximum at time = 90 min. Due to the saturation of the active sites, Q or% R was not changed when the contact time exceeded 90 min.
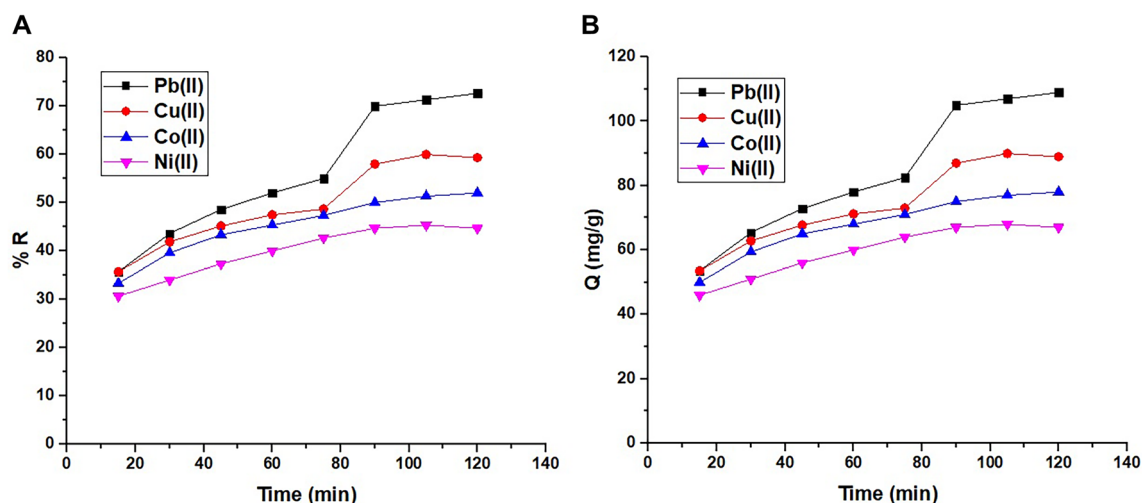
**Fig. 6** The effect of contact time of the studied metal ion solution on% R (**A**) and Q (**B**)

% R of Pb(II), Cu(II), Co(II), and Ni(II) ions at time = 90 min is 70.00, 58.00, 50.00, and 44.67, respectively. Also, Q of the composite toward Pb(II), Cu(II), Co(II), and Ni(II) ions at time = 90 min is 105.00, 87.00, 75.00, and 67.00 mg/g, respectively.

Two kinetic models, pseudo-second-order (Eq. 4) and pseudo-first-order (Eq. 5), were used to study the effect of contact time [24, 25].

$$\frac{t}{Q_t} = \frac{1}{K_2 Q_e^2} + \frac{1}{Q_e} t \tag{4}$$

$$\log(Q_e - Q_t) = logQ_e - \frac{K_1}{2.303} t \tag{5}$$

$Q_e$ (mg/g) is the composite uptake capacity toward investigated metal ions at equilibrium. $Q_t$ (mg/g) is the composite uptake capacity toward investigated metal ions at the contact time t.

The rate constant of the pseudo-first-order model is represented by $K_1$ (1/min) whereas the rate constant of the pseudo-second-order model is represented by $K_2$ (g/mg min). The pseudo-first-order and pseudo-second-order models are depicted in Fig. 7B, respectively. Table 2 shows that the correlation coefficients ($R^2$) of the pseudo-first-order model are smaller than the correlation coefficients ($R^2$) of the pseudo-second-order model. Furthermore, $Q_e$ obtained from the pseudo-second-order is more compatible with experimental uptake capacity than $Q_e$ obtained from the pseudo-first-order. As a result, the pseudo-second-order model better described the kinetic data than the pseudo-first-order model.
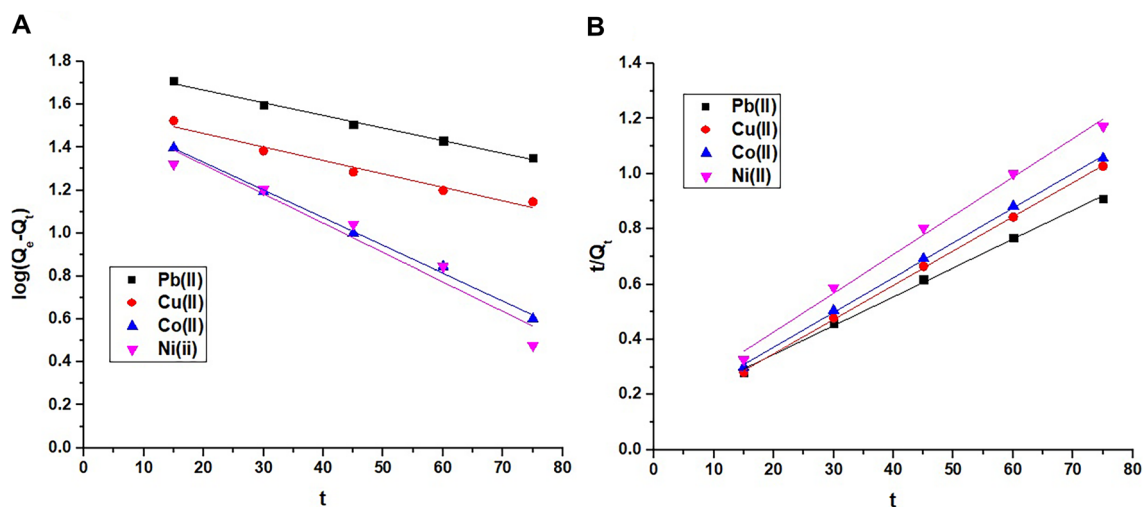


**Fig. 7** The pseudo-first-order (**A**) and pseudo-second-order (**B**) models

**Table 2** Kinetic constants

| Metal ion | Pseudo first order | | | | Pseudo second order | | | |
|---|---|---|---|---|---|---|---|---|
| | $Q_e$ (mg/g) | | $K_1$ (1/min) | $R^2$ | $Q_e$ (mg/g) | | $K_2$ (g/mg min) | $R^2$ |
| | Calculated | Experimental | | | Calculated | Experimental | | |
| Pb(II) | 61.055 | 105 | 0.0136 | 0.990 | 95.694 | 105 | 0.0008 | 0.997 |
| Cu(II) | 35.630 | 87 | 0.0144 | 0.963 | 80.710 | 87 | 0.0015 | 0.999 |
| Co(II) | 38.867 | 75 | 0.0298 | 0.995 | 79.365 | 75 | 0.0013 | 0.999 |
| Ni(II) | 39.153 | 67 | 0.0315 | 0.933 | 71.327 | 67 | 0.0014 | 0.991 |
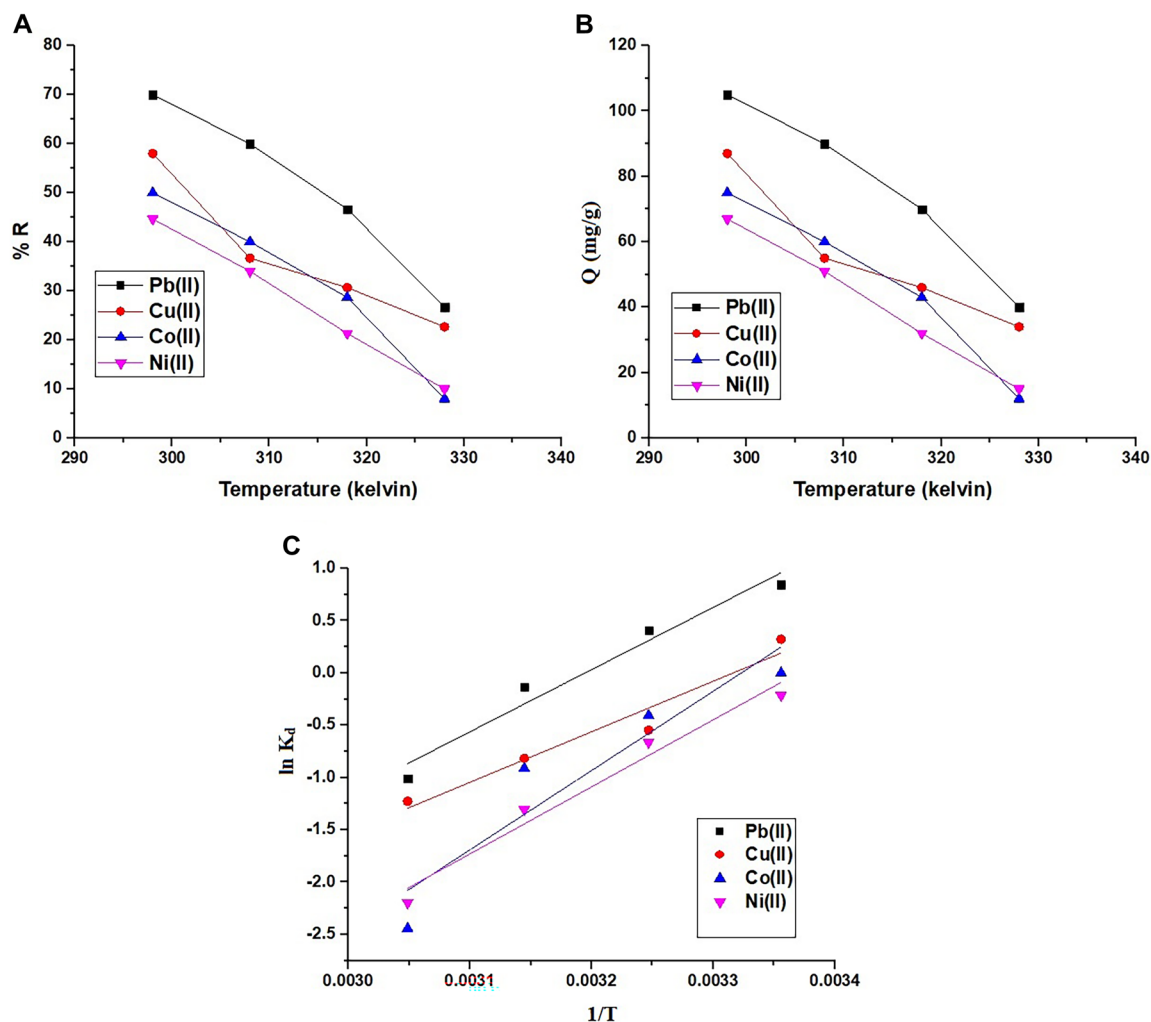


**Fig. 8** The effect of temperature of the studied metal ion solution on% R (**A**) and Q (**B**). **C** The plot of lnK$_d$ against temperature

Thus, we can say that the chemical reaction seems to play a role in the rate-controlling step.

### 3.2.3 Influence of Temperature

The effect of temperature on% R and Q (mg/g) in the examined metal ion solution is shown in Fig. 8A, B,

respectively. The data showed that as the temperature rises,% R or Q decreases until it reaches a minimum at temperature = 328 K.% R of Pb(II), Cu(II), Co(II), and Ni(II) ions at temperature = 328 K is 26.67, 22.67, 8.00, and 10.00, respectively. Also, Q of the composite toward Pb(II), Cu(II), Co(II), and Ni(II) ions at temperature = 328 K is 40.00, 34.00, 12.00, and 15.00 mg/g, respectively. As a result,

the ideal temperature is 298 K. The percentage of removal decreases when the temperature exceeds 298 K because the high heat works to return some of the adsorbed metal ions to the solution again. Equations 6, 7 were used to calculate the thermodynamic parameters such as a change in enthalpy (ΔH°), change in the entropy (ΔS°), and change in free energy (ΔG°) [24, 25].

$$lnK_d = \frac{\Delta S°}{R} - \frac{\Delta H°}{RT} \tag{6}$$

$$\Delta G° = \Delta H° - T\Delta S° \tag{7}$$

where the adsorption temperature is represented by T (Kelvin) while the distribution constant is represented by $K_d$ (L/g). In addition, R (kJ/mol kelvin) is a gas constant. Equation (8) was used to calculate the distribution constant ($K_d$) [24, 25].

$$K_d = \frac{Q_e}{C_e} \tag{8}$$

The curve of $lnK_d$ against temperature is shown in Fig. 8C. Table 3 contains all the thermodynamic parameters. Because the enthalpy value is greater than 40 kJmol, the data confirmed that the uptake of Pb(II), Cu(II), Co(II), or Ni(II) ions utilizing composite is chemical [24, 25]. Furthermore, because of the negative sign of enthalpy, the uptake of Pb(II), Cu(II), Co(II), or Ni(II) ions utilizing composite is exothermic. As demonstrated in Scheme 2, the synthesized composite can form chelates with Pb(II), Cu(II), Co(II), or Ni(II) ions. Furthermore, because of the negative sign of

free energy, the uptake of Pb(II), Cu(II), Co(II), or Ni(II) ions employing composite is spontaneous. Due to the positive sign of entropy, the uptake of Pb(II), Cu(II), Co(II), or Ni(II) ions at the solution boundary/composite takes place in a disordered manner [24, 25].

### 3.2.4 Influence of Concentration

Figure 9A, B show the influence of the examined metal ion solution concentration on% R and Q (mg/g), respectively. The results confirmed that with increasing concentration,% R drops while Q increases.% R of Pb(II), Cu(II), Co(II), and Ni(II) ions at concentration = 200 mg/L is 53.50, 44.50, 40.00, and 35.00, respectively. Also, Q of the composite toward Pb(II), Cu(II), Co(II), and Ni(II) ions at concentration = 200 mg/L is 107.00, 89.00, 80.00, and 70.00 mg/g, respectively. Two equilibrium isotherms, Freundlich (Eq. 9) and Langmuir (Eq. 10) were used to analyze the concentration data [24, 25].

$$lnQ_e = lnK_3 + \frac{1}{n}lnC_e \tag{9}$$

$$\frac{C_e}{Q_e} = \frac{1}{K_4Q_m} + \frac{C_e}{Q_m} \tag{10}$$

where $Q_m$ (mg/g) denotes the composite maximal uptake capacity. The Langmuir constant is $K_4$ (L/mg) while the Freundlich constant is $K_3$ (mg/g)(L/mg)1/n. The heterogeneity constant is represented by 1/n. Equation (11) can be used to calculate the $Q_m$ from the Freundlich isotherm [24, 25].

**Table 3** Thermodynamic parameters

| Metal ion | ΔG° (KJ/mol) | | | | ΔS° (KJ/molK) | ΔH° (KJ/mol) |
|---|---|---|---|---|---|---|
| | Temperature (Kelvin) | | | | | |
| | 298 | 308 | 318 | 328 | | |
| Pb(II) | − 97.044 | − 98.632 | − 100.220 | − 101.808 | 0.159 | − 49.717 |
| Cu(II) | − 80.354 | − 81.694 | − 83.035 | − 84.375 | 0.134 | − 40.415 |
| Co(II) | − 126.153 | − 128.259 | − 130.366 | − 132.472 | 0.211 | − 63.386 |
| Ni(II) | − 107.411 | − 109.216 | − 111.022 | − 112.828 | 0.181 | − 53.593 |

**Scheme 2** The adsorption mechanism



M= Pb(II), Cu(II), Co(II), or Ni(II)
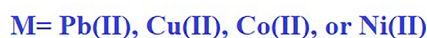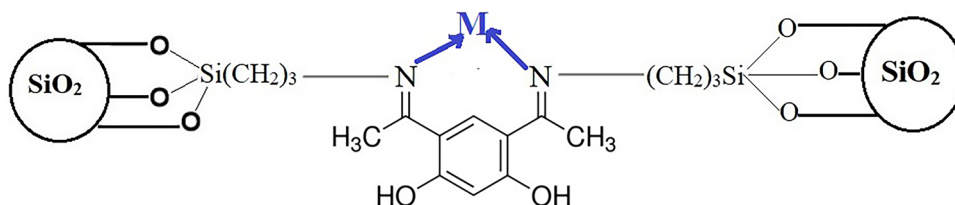
$$Q_m = K_3\left(C_i^{1/n}\right))\tag{11}$$

The Langmuir and Freundlich isotherms are depicted in Fig. 10A, B, respectively. The data revealed that the

Freundlich isotherm correlation coefficients ($R^2$) are lower than those of Langmuir as shown in Table 4. As a result, the Langmuir isotherm was better at describing the equilibrium data than the Freundlich isotherm. The maximum uptake capacity of the composite toward Pb(II), Cu(II), Co(II), or
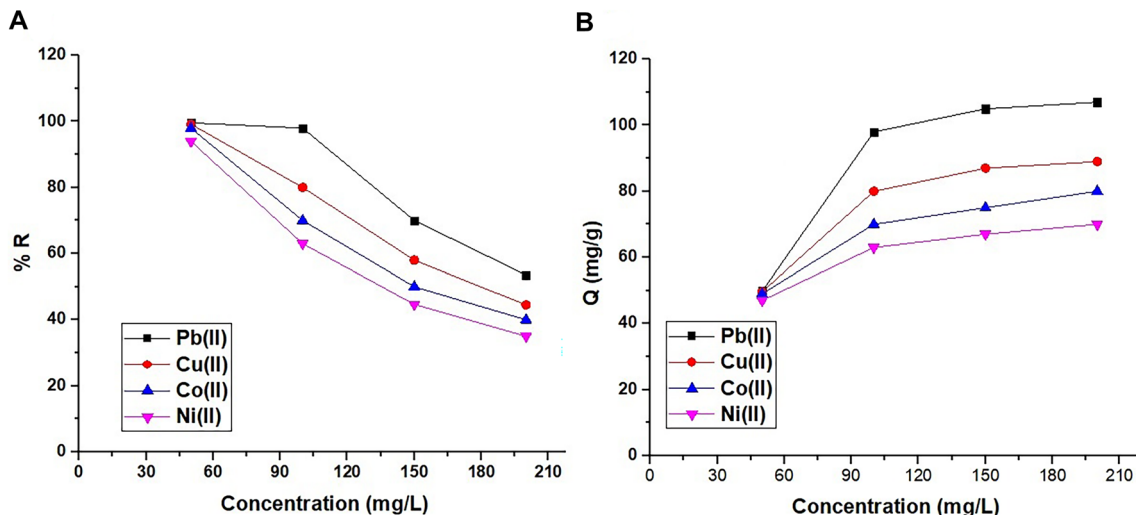
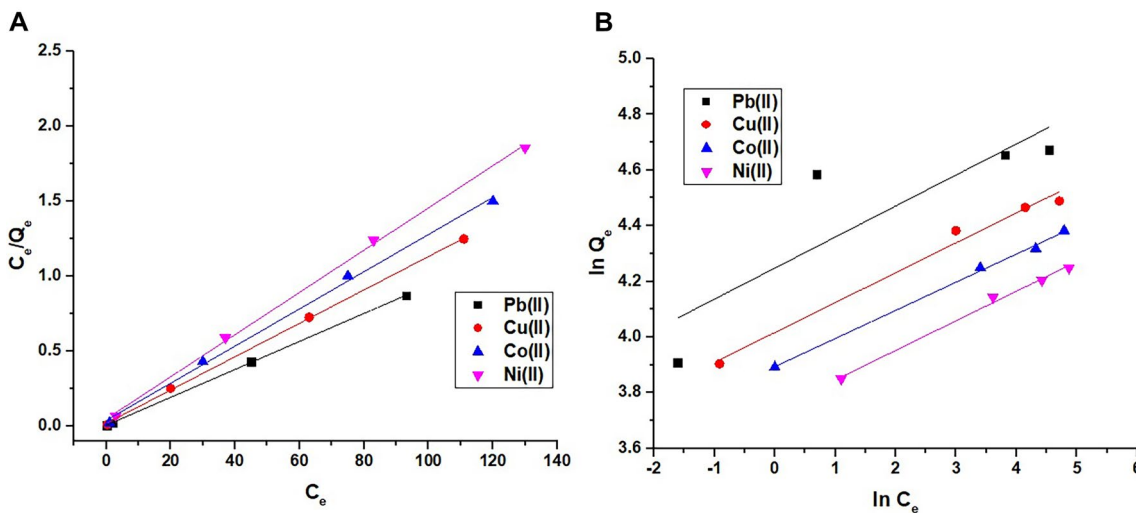**Fig. 9** The effect of concentration of the studied metal ion solution on% R (**A**) and Q (**B**)

**Fig. 10** The Langmuir (**A**) and Freundlich (**B**) isotherms

**Table 4** Equilibrium constants

| Metal ion | Langmuir | | | Freundlich | | |
|---|---|---|---|---|---|---|
| | $Q_m$ (mg/g) | $K_3$ (L/mg) | $R^2$ | $Q_m$ (mg/g) | $K_4$ (mg/g) (L/mg)$^{1/n}$ | $R^2$ |
| Pb(II) | 107.066 | 3.199 | 0.999 | 122.371 | 69.953 | 0.628 |
| Cu(II) | 89.767 | 0.709 | 0.999 | 95.115 | 55.492 | 0.978 |
| Co(II) | 80.580 | 0.346 | 0.997 | 81.495 | 49.090 | 0.996 |
| Ni(II) | 70.972 | 0.311 | 0.998 | 71.704 | 42.063 | 0.991 |

**Table 5** A comparative study between the adsorption capacity of the composite with other materials
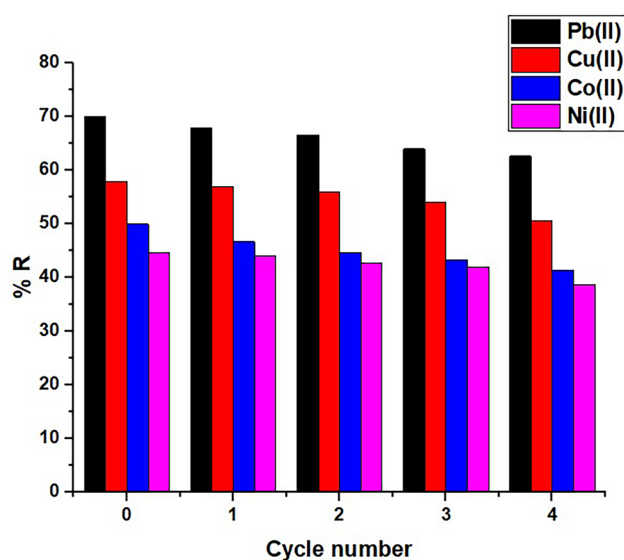
| Adsorbent | Q (mg/g) toward Cu(II) ions | Q (mg/g) toward Pb(II) ions | Q (mg/g) toward Co(II) ions | Q (mg/g) toward Ni(II) ions | Refs. |
|---|---|---|---|---|---|
| Graft copolymer of chitosan with 2-acrylamido-2-methyl-1-propanesulfonic acid | – | – | – | 32.74 | [42] |
| Iron oxide/chitosan composite | – | – | – | 1.140 | [42] |
| Zeolite modified with 4-(3-triethoxysilylpropyl) thiosemicarbazide | 29.50 | – | 24.90 | 16.60 | [43] |
| Montmorillonite | 9.58 | 54.49 | 12.08 | – | [44] |
| Guanyl-modified cellulose | 83.00 | 52.00 | – | – | [45] |
| Carbon gels | 6.64 | 16.95 | 5.46 | 4.16 | [46] |
| $Fe_3O_4$ | – | – | 17.40 | – | [47] |
| Thiol–ended polycaprolactone | – | 10.35 | – | – | [48] |
| $SiO_2$/Schiff base composite | 107.066 | 89.767 | 80.580 | 70.972 | This study |
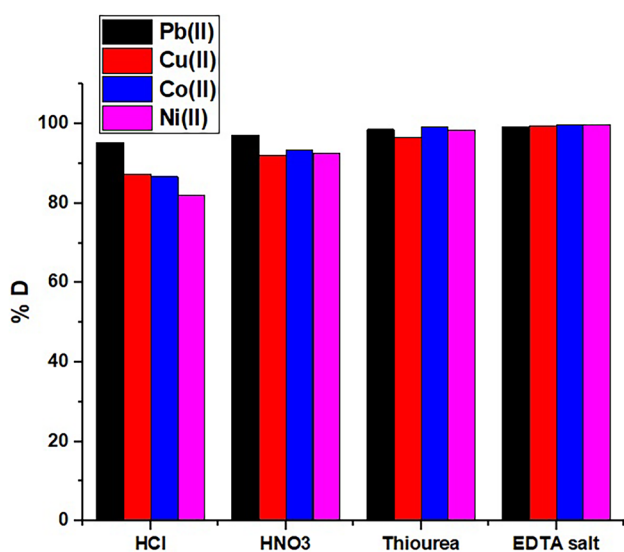


**Fig. 11** The plot of% D against some desorbing solutions



**Fig. 12** The plot of% R against the cycle number

Ni(II) ions is 107.066, 89.767, 80.580, and 70.972 mg/g, respectively. As shown in Table 5 [42–48], the uptake capacity of the synthesized composite was compared to that of other adsorbents such as graft copolymer, iron oxide/chitosan composite, carbon gels, modified zeolite with 4-(3-triethoxysilylpropyl)thiosemicarbazide, montmorillonite, guanyl-modified cellulose, mercaptotriazole-functionalized nickel-zin, $Fe_3O_4$, and thiol–ended polycaprolactone. Because of its high adsorption capacity, the synthesized composite outperformed most of the adsorbents.

### 3.2.5 Influence of Desorption and Reusability

The plot of% D against different desorbing solutions is shown in Fig. 11. 0.45 M hydrochloric acid, nitric acid, thiourea, and EDTA disodium salt were utilized as desorbing solutions. The results showed that 0.45 M of EDTA disodium salt is the best desorbing solution for recovering the largest amount of metal ions from the synthesized composite. EDTA is the head member of the family of ligands. EDTA is a hexadentate ligand forming highly stable complexes with Pb(II), Cu(II), Co(II), and Ni(II) ions in an aqueous solution. So, it has the affinity to uptake these metal ions from the composite surface. The plot of% R against the cycle number is shown in Fig. 12. The small decrease in% R demonstrates that the synthesized composite can be regenerated and reused efficiently in the uptake of Pb(II), Cu(II), Co(II), and Ni(II) ions from aqueous solutions.

# 4 Conclusions

By modifying silica nanoparticles with 4,6-diacetylresorcinol, a new composite was created. XRD, FT-IR, FE-SEM, $N_2$ adsorption/desorption analyzer, and CHN analyzer were used to characterize the synthesized composite. Pb(II), Cu(II), Co(II), and Ni(II) ions were efficiently removed from aqueous solutions using the produced composite. The maximum uptake capacity of the composite toward Pb(II), Cu(II), Co(II), or Ni(II) ions is 107.066, 89.767, 80.580, and 70.972 mg/g, respectively. The results showed that at pH 6.5, contact time = 90 min, and adsorption temperature = 298 K, the greatest% removal of examined metal ions was attained.

## Declarations

**Conflict of interest** The authors confirm that there is no conflict of interest for this paper.

## References

1. M. Sultana, M.H. Rownok, M. Sabrin, M.H. Rahaman, S.M.N. Alam, A review on experimental chemically modified activated carbon to enhance dye and heavy metals adsorption. Clean. Eng. Technol. **6**, 100382 (2022)

2. J. Li, Z. Lei Yang, T. Ding, Y.J. Song, H.C. Li, D. Qiang Li, S. Chen, F. Xu, The role of surface functional groups of pectin and pectin-based materials on the adsorption of heavy metal ions and dyes. Carbohydr. Polym. **276**, 118789 (2022)

3. U.O. Aigbe, K.E. Ukhurebor, R.B. Onyancha, O.A. Osibote, H. Darmokoesoemo, H.S. Kusuma, Fly ash-based adsorbent for adsorption of heavy metals and dyes from aqueous solution: a review. J. Mater. Res. Technol. **14**, 2751–2774 (2021)

4. E.A. Abdelrahman, R.M. Hegazey, R.E. El-Azabawy, Efficient removal of methylene blue dye from aqueous media using Fe/Si, Cr/Si, Ni/Si, and Zn/Si amorphous novel adsorbents. J. Mater. Res. Technol. **8**, 5301–5313 (2019)

5. R.M. Hegazey, E.A. Abdelrahman, Y.H. Kotp, A.M. Hameed, A. Subaihi, Facile fabrication of hematite nanoparticles from Egyptian insecticide cans for efficient photocatalytic degradation of rhodamine B dye. J. Mater. Res. Technol. **9**, 1652–1661 (2020)

6. N.H. Abdullah, K. Shameli, E.C. Abdullah, L.C. Abdullah, Solid matrices for fabrication of magnetic iron oxide nanocomposites: synthesis, properties, and application for the adsorption of heavy metal ions and dyes. Compos. Part B Eng. **162**, 538–568 (2019)

7. M.T. ALSamman, J. Sánchez, Recent advances on hydrogels based on chitosan and alginate for the adsorption of dyes and metal ions from water. Arab. J. Chem. **14**, 102455 (2021)

8. S. Dubey, M. Shri, A. Gupta, V. Rani, D. Chakrabarty, Toxicity and detoxification of heavy metals during plant growth and metabolism. Environ. Chem. Lett. **16**, 1169–1192 (2018)

9. S.R. Mallampati, Y. Mitoma, T. Okuda, S. Sakita, M. Kakeda, Total immobilization of soil heavy metals with nano-Fe/Ca/CaO dispersion mixtures. Environ. Chem. Lett. **11**, 119–125 (2013)

10. E.R. Sumner, A. Shanmuganathan, T.C. Sideri, S.A. Willets, J.E. Houghton, S.V. Avery, Oxidative protein damage causes chromium toxicity in yeast. Microbiology **151**, 1939–1948 (2005)

11. M. Słota, M. Wąsik, T. Stołtny, A. Machoń-Grecka, S. Kasperczyk, Effects of environmental and occupational lead toxicity and its association with iron metabolism. Toxicol. Appl. Pharmacol. **434**, 115794 (2022)

12. G. Pascual, D. Sano, T. Sakamaki, M. Akiba, O. Nishimura, The water temperature changes the effect of pH on copper toxicity to the green microalgae Raphidocelis subcapitata. Chemosphere **291**, 133110 (2022)

13. G.K. Macoustra, D.F. Jolley, J.L. Stauber, D.J. Koppel, A. Holland, Speciation of nickel and its toxicity to Chlorella sp. in the presence of three distinct dissolved organic matter (DOM). Chemosphere **273**, 128454 (2021)

14. V. Verougstraete, R. Danzeisen, V. Viegas, P. Marsh, A. Oller, A tiered approach to investigate the inhalation toxicity of cobalt substances. Tier 1: bioaccessibility testing. Regul. Toxicol. Pharmacol. **129**, 105124 (2022)

15. A.K. Sinha, V. Matey, T. Giblen, R. Blust, G. De Boeck, Gill remodeling in three freshwater teleosts in response to high environmental ammonia. Aquat. Toxicol. **155**, 166–180 (2014)

16. L.A. Malik, A. Bashir, A. Qureashi, A.H. Pandith, Detection and removal of heavy metal ions: a review. Environ. Chem. Lett. **17**, 1495–1521 (2019)

17. E.A. Abdelrahman, Y.G. Abou El-Reash, H.M. Youssef, Y.H. Kotp, R.M. Hegazey, Utilization of rice husk and waste aluminum cans for the synthesis of some nanosized zeolite, zeolite/zeolite, and geopolymer/zeolite products for the efficient removal of Co(II), Cu(II), and Zn(II) ions from aqueous media. J. Hazard. Mater. **401**, 123813 (2021)

18. M.A. Barakat, New trends in removing heavy metals from industrial wastewater. Arab. J. Chem. **4**, 361–377 (2011)

19. Y. Sun, S. Zhou, W. Sun, S. Zhu, H. Zheng, Flocculation activity and evaluation of chitosan-based flocculant CMCTS-g-P(AM-CA) for heavy metal removal. Sep. Purif. Technol. **241**, 116737 (2020)

20. W. Zeng, W. Guo, B. Li, Z. Wei, D.D. Dionysiou, R. Xiao, Kinetics and mechanistic aspects of removal of heavy metal through gas-liquid sulfide precipitation: a computational and experimental study. J. Hazard. Mater. **408**, 124868 (2021)

21. Y. Ding, J. Wu, J. Wang, J. Wang, J. Ye, F. Liu, Superhydrophilic carbonaceous-silver nanofibrous membrane for complex oil/water separation and removal of heavy metal ions, organic dyes and bacteria. J. Memb. Sci. **614**, 118491 (2020)

22. P. Wu, X. Wu, Y. Wang, H. Xu, G. Owens, A biomimetic interfacial solar evaporator for heavy metal soil remediation. Chem. Eng. J. **435**, 134793 (2022)

23. S. Pan, J. Shen, Z. Deng, X. Zhang, B. Pan, Metastable nanozirconium phosphate inside gel-type ion exchanger for enhanced removal of heavy metals. J. Hazard. Mater. **423**, 127158 (2022)

24. E.A. Abdelrahman, A. Alharbi, A. Subaihi, A.M. Hameed, M.A. Almutairi, F.K. Algethami, H.M. Youssef, Facile fabrication of novel analcime/sodium aluminum silicate hydrate and zeolite Y/faujasite mesoporous nanocomposites for efficient removal of Cu(II) and Pb(II) ions from aqueous media. J. Mater. Res. Technol. **9**, 7900–7914 (2020)

25. A.M. Hameed, A. Alharbi, E.A. Abdelrahman, E.M. Mabrouk, R.M. Hegazey, F.K. Algethami, Y.O. Al-Ghamdi, H.M. Youssef, Facile hydrothermal fabrication of analcime and zeolite X for

efficient removal of Cd(II) ions from aqueous media and polluted water. J. Inorg. Organomet. Polym. Mater. **30**, 4117–4128 (2020)

26. E.A. Abdelrahman, R.M. Hegazey, Utilization of waste aluminum cans in the fabrication of hydroxysodalite nanoparticles and their chitosan biopolymer composites for the removal of Ni(II) and Pb(II) ions from aqueous solutions: kinetic, equilibrium, and reusability studies. Microchem. J. **145**, 18–25 (2019)

27. E.A. Abdelrahman, R.M. Hegazey, Exploitation of Egyptian insecticide cans in the fabrication of Si/Fe nanostructures and their chitosan polymer composites for the removal of Ni(II), Cu(II), and Zn(II) ions from aqueous solutions. Compos. Part B Eng. **166**, 382–400 (2019)

28. M.E. Khalifa, E.A. Abdelrahman, M.M. Hassanien, W.A. Ibrahim, Application of mesoporous silica nanoparticles modified with dibenzoylmethane as a novel composite for efficient removal of Cd(II), Hg(II), and Cu(II) ions from aqueous media. J. Inorg. Organomet. Polym. Mater. **30**, 2182–2196 (2020)

29. E.A. Abdelrahman, A. Subaihi, Application of geopolymers modified with chitosan as novel composites for efficient removal of Hg(II), Cd(II), and Pb(II) ions from aqueous media. J. Inorg. Organomet. Polym. Mater. **30**, 2440–2463 (2020)

30. M. Adibmehr, H. Faghihian, Magnetized activated carbon prepared by oak shell biowaste and modified with nickel hexacyanoferrate for selective removal of cesium. J. Inorg. Organomet. Polym. Mater. **29**, 1941–1955 (2019)

31. I.O. Ali, S.M. El-Sheikh, T.M. Salama, E.K. Abdel-Khalek, M.S. Thabet, M.F. Bakr, M.H. Fodial, Novel composites of multifunctional NaP zeolite/graphene oxide for highly efficient removal of Fe(III) from aqueous solution. J. Inorg. Organomet. Polym. Mater. **31**, 577–590 (2021)

32. M. Dinari, N. Roghani, Calcium iron layered double hydroxide/ poly(vinyl chloride) nanocomposites: synthesis, characterization and Cd2+ removal behavior. J. Inorg. Organomet. Polym. Mater. **30**, 808–819 (2020)

33. A.T. Hoang, S. Nižetić, C.K. Cheng, R. Luque, S. Thomas, T.L. Banh, V.V. Pham, X.P. Nguyen, Heavy metal removal by biomassderived carbon nanotubes as a greener environmental remediation: a comprehensive review. Chemosphere **287**, 131959 (2022)

34. A.M. Naglah, M.A. Al-Omar, A.A. Almehizia, H.M. AlKahtani, A.J. Obaidullah, M.A. Bhat, N.S. Al-Shakliah, Application of nanosized zeolite X modified with glutamic acid as a novel composite for the efficient removal of Co(II) ions from aqueous media. J. Inorg. Organomet. Polym. Mater. **31**, 2105–2115 (2021)

35. S. Rahpeima, V. Javanbakht, J. Esmaili, Synthesis and characterization of activated carbon/maghemite/starch magnetic bionanocomposite and its application for permanganate removal from aqueous solution. J. Inorg. Organomet. Polym. Mater. **28**, 195–211 (2018)

36. H.S. Far, M. Hasanzadeh, M. Najafi, T.R.M. Nezhad, M. Rabbani, Efficient removal of Pb(II) and Co(II) ions from aqueous solution with a chromium-based metal-organic framework/activated carbon composites. Ind. Eng. Chem. Res. **60**, 4332–4341 (2021)

37. H.S. Far, M. Hasanzadeh, M.S. Nashtaei, M. Rabbani, Fast and efficient adsorption of palladium from aqueous solution by magnetic metal–organic framework nanocomposite modified with poly(propylene imine ) dendrimer. Environ. Sci. Pollut. Res. **28**, 62474–62486 (2021)

38. S. Xue, H. Xie, H. Ping, Q. Li, B. Su, Z. Fu, Induced transformation of amorphous silica to cristobalite on bacterial surface. RSC Adv. **88**, 1–11 (2015)

39. V. Correcher, J. Garcia-Guinea, M.A. Bustillo, R. Garcia, Study of the thermoluminescence emission of a natural α-cristobalite. Radiat. Eff. Defects Solids **164**, 59–67 (2009)

40. Z.P. Xu, P.S. Braterman, High affinity of dodecylbenzene sulfonate for layered double hydroxide and resulting morphological changes. J. Mater. Chem. **13**, 268–273 (2003)

41. A.E. Shalapy, Y.G. Abou El-Reash, E.A. Abdelrahman, M.E. Khalifa, Facile synthesis and characterisation of novel Sn/Si mixtures for the efficient removal of methylene blue and crystal violet dyes from aqueous media. Int. J. Environ. Anal. Chem. (2021). https://doi.org/10.1080/03067319.2021.1986036

42. R.K. Shah, A.M. Naglah, M.A. Al-Omar, A.A. Almehizia, S. AlReshaidan, A. Subaihi, A. Alharbi, A.M. Hameed, J. Alkabli, M.E. Fetoh, A.A. Alluhaybi, A.S. Al-Wasidi, T.S. Alraddadi, H.M. Youssef, Efficient removal of Ni(II) ions from aqueous solutions using analcime modified with dimethylglyoxime composite. Arab. J. Chem. **14**, 103197 (2021)

43. S.N. Adamovich, E.G. Filatova, Y.N. Pozhidaev, I.A. Ushakov, A.D. Chugunov, E.N. Oborina, I.B. Rozentsveig, F. Verpoort, Natural zeolite modified with 4-(3-triethoxysilylpropyl) thiosemicarbazide as an effective adsorbent for Cu(II), Co(II) and Ni(II). J. Taiwan Inst. Chem. Eng. **129**, 396–409 (2021)

44. C. Chen, H. Liu, T. Chen, D. Chen, R.L. Frost, An insight into the removal of Pb(II), Cu(II), Co(II), Cd(II), Zn(II), Ag(I), Hg(I), Cr(VI) by Na(I)-montmorillonite and Ca(II)-montmorillonite. Appl. Clay Sci. **118**, 239–247 (2015)

45. I.M. Kenawy, M.A.H. Hafez, M.A. Ismail, M.A. Hashem, Adsorption of Cu(II), Cd(II), Hg(II), Pb(II) and Zn(II) from aqueous single metal solutions by guanyl-modified cellulose. Int. J. Biol. Macromol. **107**, 1538–1549 (2018)

46. M. Osińska, Removal of lead(II), copper(II), cobalt(II) and nickel(II) ions from aqueous solutions using carbon gels. J. SolGel Sci. Technol. **81**, 678–692 (2017)

47. A. Uheida, G. Salazar-Alvarez, E. Björkman, Z. Yu, M. Muhammed, Fe3O4 and γ-Fe$_2$O$_3$ nanoparticles for the adsorption of Co$^{2+}$ from aqueous solution. J. Colloid Interface Sci. **298**, 501–507 (2006)

48. B. Körpınar, A. Erdem Yayayürük, O. Yayayürük, H. Akat, Thiol–ended polycaprolactone: synthesis, preparation and use in Pb(II) and Cd(II) removal from water samples. Mater. Today Commun. **29**, 102908 (2021)